JOURNAL OF MATERIALS SCIENCE **39** (2004) 6439–6447

Control of the particle size and morphology of hydrothermally synthesised lead zirconate titanate powders

B. SU, T. W. BUTTON, C. B. PONTON
IRC in Materials Processing, Department of Metallurgy and Materials, School of Engineering, The University of Birmingham, Edgbaston, Birmingham B15 2TT, UK
E-mail: b.su@bham.ac.uk

The particle size and morphology of hydrothermally synthesised lead zirconate titanate (PZT) powders can be controlled by concentrations of the mineraliser such as potassium hydroxide (KOH), and the hydrothermal synthesis temperature and time, which all influence the particle nucleation and growth mechanisms. The mineraliser is crucial in facilitating both the *in-situ* transformation process during the nucleation stage and the nuclei-coagulation process during the subsequent growth stage. Its concentration must be high enough to ensure the formation of only pure perovskite PZT particles but low enough to prevent excessive PZT particle growth. The minimum necessary mineraliser concentration has, however, strong dependence on both the hydrothermal synthesis temperature and chemical environment in hydrothermal solution. Thus, perovskite PZT powders with ca. 200 nm particle size and narrow particle size distribution can be synthesised hydrothermally at 300°C using KOH as a mineraliser with a minimum concentration of 0.4 M.

1. Introduction

Lead zirconate titanate (PZT) is one of the most commonly used ferroelectric ceramic materials. The conventional route for fabricating such a ceramic encounters several processing problems, such as chemical imhomogeneity and a non-uniform microstructure, as a result of the particle agglomeration, evaporation of lead, etc. during various processing stages. Given that powders with a submicron particle size and a narrow particle size distribution are regarded as being beneficial for ceramic processing, and that the benefits of using colloidally stable, submicron-sized powders in the fabrication of uniform microstructure ceramics are now becoming widely recognised [1], alternative powder synthesis and processing routes are being sought. Hydrothermal powder synthesis is reported to be a superior chemical preparation route for multi-cation oxide ceramic powders compared with the conventional mixed-oxide route [2, 3]. This is because crystalline ceramic powders can be formed directly from the precursor solution at relatively low temperatures (typically $\leq 300^{\circ}C$), which are much lower than those required in the conventional solid-state reaction process. This feature is of particular importance when making high quality, reliable PZT ceramics since the lead component is particularly volatile at temperatures above 800°C. Therefore, this wet chemical route has been investigated extensively for the synthesis of PZT powders and thin films in the last decades [4–9]. Most of the studies, however, have concentrated on determining the synthesis conditions for perovskite PZT phase formation, with little consideration being given to the control of resultant powder particle size distribution and morphology during hydrothermal synthesis [10, 11]. Few studies have been investigated on the PZT particle growth mechanism in terms of the hydrothermal solution chemistry [12] and the formation mechanism of the intermediate products [13].

In this paper, the hydrothermal synthesis conditions for perovskite PZT powders have been investigated. The effects of the mineraliser, the synthesis temperature and time, on phase formation, particle size, and particle morphology are considered. Control of the particle size and morphology of the hydrothermal PZT powders is then discussed with reference to the proposed formation mechanism [13] of perovskite PZT powders during hydrothermal synthesis.

2. Experimental procedure

2.1. Materials

The starting materials for the preparation of the feedstock were lead acetate trihydrate, $Pb(CH_3COO)_2{\cdot}3H_2O$ [denoted as $Pb(OAc)_2{\cdot}3H_2O$, from Fluka, UK]; zirconium acetate solution [denoted as $ZrO(OAc)_2$, from MEL Chemicals, UK, containing the equivalent of 22.5 wt% ZrO_2 and 17.0 wt% CH_3COO^- according to the manufacturer's specifications]; and tetra-iso-propyltitanate, $Ti(OCH(CH_3)_2)_4$ [denoted as TIPT, from Tioxide, UK]. The TIPT was first modified

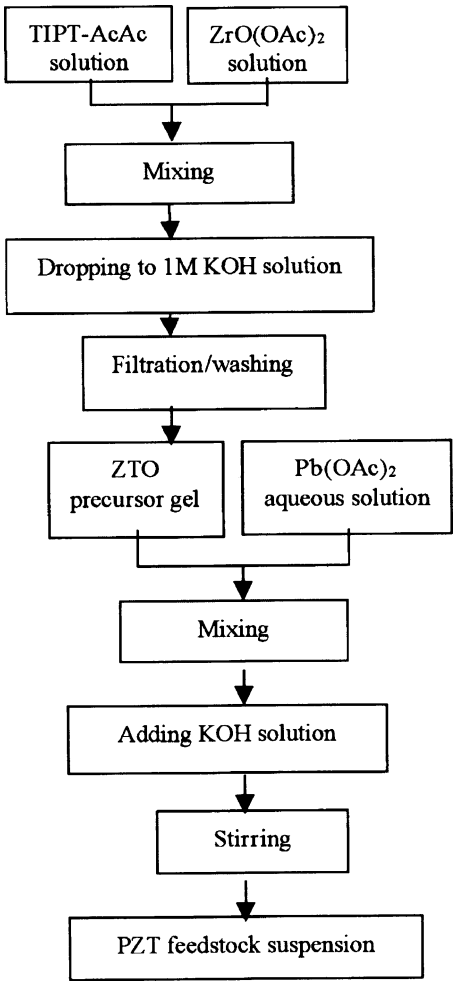

Figure 1 Flow chart of hydrothermal feedstock preparation procedure.

by adding acetylacetone [denoted as AcAc, from Aldrich, UK] to it at room temperature in the molar ratio of 2 AcAc to 1 TIPT, with continual stirring for 4 h. This addition is to stabilise the metal alkoxide against precipitation or gelation.

The feedstock for hydrothermal synthesis was prepared as shown in Fig. 1. A zirconia-titania precursor gel was prepared initially by mixing the zirconia and titania precursor solutions together, and then adding the resultant solution dropwise into a 1 M KOH aqueous solution to ensure the simultaneous precipitation of each cation. The co-precipitate was then washed with deionised water and filtered off. Finally, the washed zirconia-titania precursor gel was mixed with lead precursor solution in the ratio of $Pb/(Ti + Zr) = 1$ and theoretically necessary to obtain the desired $Pb(Zr_{0.52}Ti_{0.48})O_3$ composition. The molarity of resultant PZT feedstock solution was 0.2 M. KOH mineraliser with concentrations ranging from 0.2 to 1.0 M were used in the hydrothermal PZT powder synthesis experiments.

2.2. Hydrothermal synthesis

Hydrothermal synthesis of the PZT powders was performed under autogenous pressure, either in a PTFE-lined 250 ml autoclave equipped with a magnetic stirrer/follower system (Berghof, Germany) or in a 4 litre corrosion-resistant nickel-base superalloy (HASTELLOY C276) autoclave equipped with a mechanically-driven magnetically-coupled stirring unit (Baskerville, UK) depending on the chosen synthesis temperatures. A constant stirring rate of 500 revolutions per minute and a constant heating rate of 3°C/min were used. Synthesis temperatures varied from 100 to 350°C, with holding times ranging from 10 min to 48 h. The pressure build-up in the autoclave as a function of temperature is shown in Fig. 2. Samples of the reaction products were extracted through a specially designed valve at various temperatures and times during the synthesis process. The solid portion was separated from the extracted suspensions by centrifugation or sedimentation. The resulting PZT powders were washed with deionised water several times until the powder suspensions became pH-neutral; then separated from solution by centrifuging or sedimentation; and finally freeze-dried. The pH was measured by a calibrated Gallenhamp pH stickmeter.

2.3. Powder characterisation

The surface charge of the hydrothermal PZT powders was characterised by measuring the particle electrophoretic mobility. Measurements were conducted

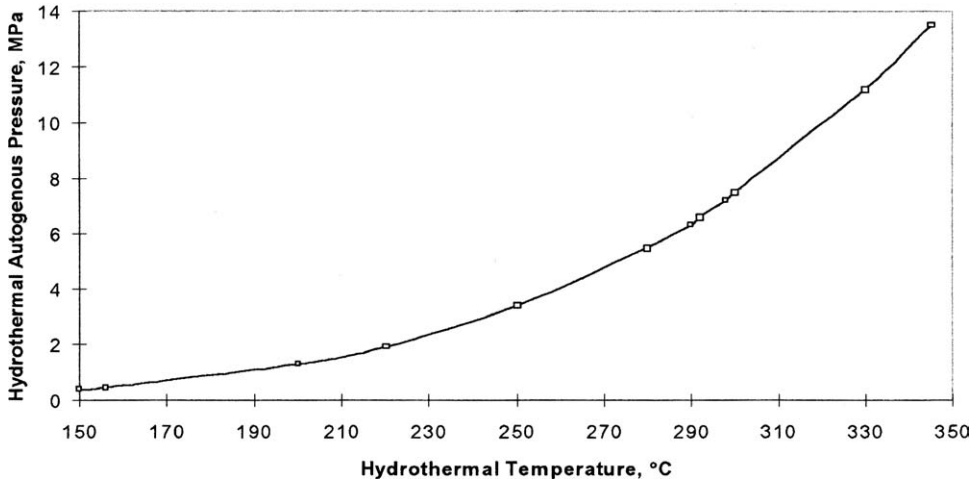

Figure 2 The dependence of the autogeneous pressure on the hydrothermal temperature.

on a Doppler electrophoretic light scattering analyser (Coulter Delsa 440) using 1 vol% powder suspension samples. All measurements were done in the presence of 0.01 M KNO_3 aqueous solution in order to suppress the effect of the counter-ions on the particle electrophoretic mobility. The pH was adjusted by the addition of dilute (0.1 M) KOH or HNO_3 solution.

X-ray diffractometry (XRD) analysis was performed on a Philips PW 1710 X-ray diffractometer using nickel-filtered monochromatic Cu K_α radiation at 40 kV and 30 mA with degree steps of 0.05° 2θ and count time of 1 s per step. Qualitative phase identification was carried out by visual comparison of patterns to JCPDS standards. Quantitative XRD was performed by using silicon as an internal standard. Calibration curves were established by mixing a fully crystallised PZT powder and a hydrothermally synthesised amorphous PZT powder at different weight ratios (1.0:0, 0.75:0.25, 0.5:0.5, 0.25:0.75, 0:1.0) with 20 wt% Si powder and calculating the ratios of area between PZT [110] and Si [111] using PC-APD software. The degree of conversion of hydrothermally synthesised powder was then derived from the PZT [110]/Si [111] peak area ratio of the hydrothermal products at various stages which were mixed mechanically with 20 wt% Si powder using a mortal and pestle.

The particle size distribution was measured using a Coulter LS 130 laser diffraction particle size analyser. Both differential and cumulative particle size distributions were calculated in terms of the number and volume percentage. The powder morphology and chemical composition were also characterised by transmission electron microscopy (TEM) combined with X-ray energy dispersive spectroscopy (EDS) analysis (Philips CM20 TEM with a Link 6586 EDS analyser) and scanning electron microscopy (SEM) using a Jeol 5410 SEM.

3. Experimental results

3.1. Hydrothermal synthesis conditions for perovskite PZT formation

From the thermodynamic point of view, the conversion of PZT precursors into PZT powders under hydrothermal conditions can be written as

$$Pb^{2+} + xTiO_2 + (1-x)ZrO_2 + 2OH^- \Leftrightarrow PbTi_xZr_{1-x}O_3 + H_2O \quad (1)$$

From Equation 1, we can see that the molar ratio between Pb precursor and mineraliser KOH should be 0.5 to complete the above reaction. In this work, the initial molar concentration of lead acetate is 0.2 M, thus the minimum amount of KOH should be 0.4 M. Fig. 3 shows the degree of conversion of hydrothermal products derived from different synthesis temperatures using 0.4 and 0.8 M KOH as the mineraliser. It can be seen that the conversion processes become rapid when the temperature approaches 300°C. Higher degree of conversion has been obtained when using 0.8 M KOH. Its degree of conversion is ca. 80% while ca. 60% is obtained when using 0.4 M KOH at the same temperature

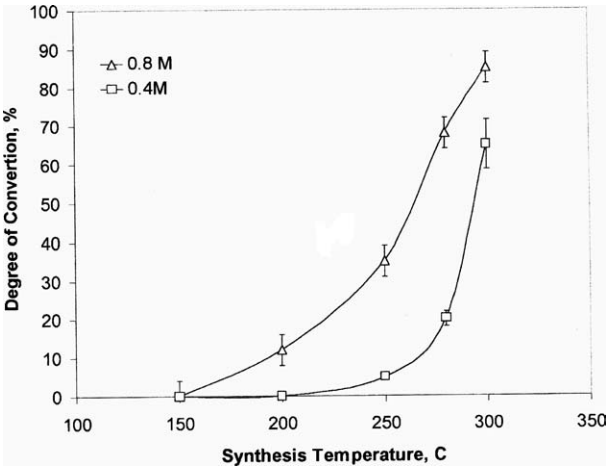

Figure 3 Degree of conversion of hydrothermal PZT determined by XRD as a function of synthesis temperature at different mineraliser concentrations.

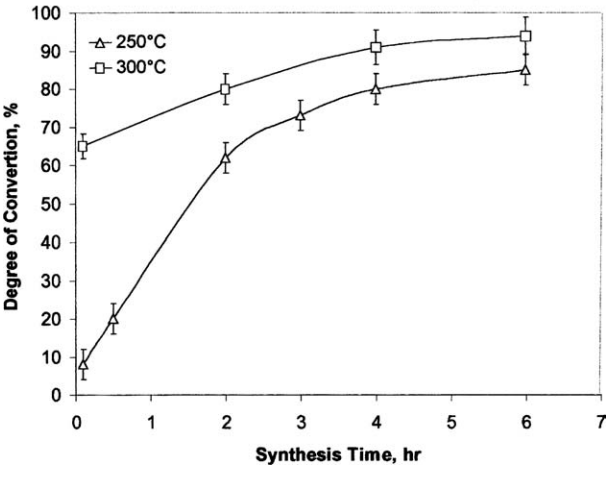

Figure 4 Degree of conversion of hydrothermal PZT determined by XRD as a function of synthesis time at different synthesis temperatures.

(300°C). As the time increases, the conversion process continues as shown in Fig. 4. The degree of conversion is ca. 90% when synthesis time is 4 h. But clearly, most of the reactions take place in the first 2 h. At lower temperature of 250°C, the conversion process is much slower, longer time is needed to obtain the same degree at higher synthesis temperatures.

Fig. 5 shows a temperature-time diagram for the formation of hydrothermal PZT powders. At temperatures up to 150°C and 2 h, the hydrothermal products are amorphous. Elevated temperatures >200°C and/or longer reaction times facilitate the transformation from amorphous to perovskite PZT phase. However, intermediate phases such as $PbTiO_3$, PbO and TiO_2 were found to co-exist with the perovskite PZT phase and some amorphous phases having non-stoichiometric PZT compositions (as indicated by TEM EDS analysis). The presence of such phases was found to depend markedly on the mineraliser concentration used. When the concentration of the mineraliser is higher than its required one for stoichiometric PZT phase formation at the chosen synthesis temperatures, the multi-phase region becomes much narrower and the perovskite PZT phase is formed more rapidly from the amorphous phases.

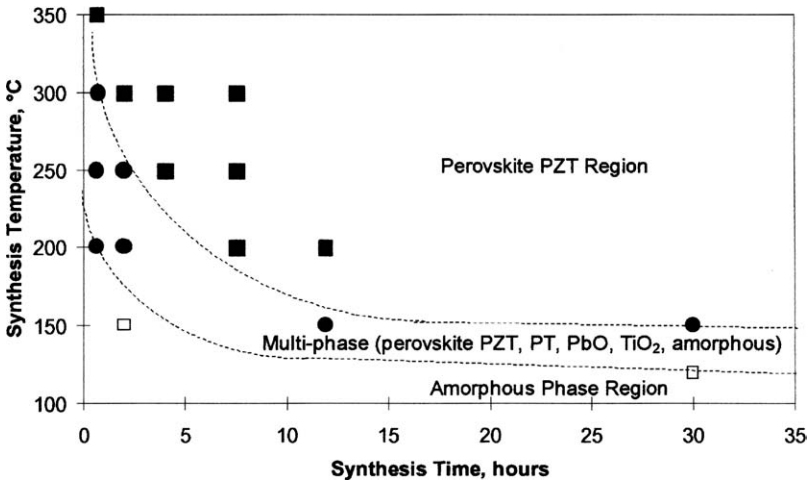

Figure 5 A tentative temperature-time phase formation diagram for powders synthesised hydrothermally using 0.4 M KOH as a mineraliser. The dashed lines represent nominal temperature-time boundaries for the perovskite PZT phase (■), multi-phase (●), and amorphous phase (□) regions.

3.2. Effect of hydrothermal synthesis conditions on the particle size and morphology of PZT powders

Fig. 6 shows SEM micrographs of the PZT powders synthesised at 300°C for 2 h using KOH as a mineraliser at different molar concentrations together with the one-step derived feedstock. As the KOH concentration increases from 0.4 to 1.0 M, both the particle size and the extent of particle agglomeration increase significantly. The morphology of the PZT powder changes from comprising definitely cubic particles at lower mineraliser concentrations to comprising increasingly large spherical cubic PZT particle agglomerates (of larger and less obviously cubic particles) at higher mineraliser concentrations. It can also be seen from Fig. 7a and b that increasing the KOH concentration from 0.4 to 0.6 M results in the particle size distribution becoming narrower but shifting to a larger particle size, with the modal particle size increasing from 0.37 to 0.71 μm. Increasing the mineraliser molar concentration from 0.6 to 1.0 M in 0.2 M steps increases the distribution modal particle size in increments of about 0.25 μm to a modal particle size of 1.22 μm at a 1.0 M KOH concentration, although the distribution widths remain more or less the same. A similar trend was shown by the volume % particle size distribution curves. The modal sizes for both the "elementary particles" as represented by number % and the "particle agglomerates" as represented by volume %, increase with the mineraliser concentration as shown in Fig. 8.

The effect of the synthesis temperature and time at a given KOH mineraliser molar concentration on the particle size distribution is summarised in Table I. First, comparing the particle size data for a synthesis temperature of 250°C and synthesis time of 2, 4 and 6 h, in terms of the "elementary" particle size (see number % data in Table I) and the "particle agglomerate" size (as represented by the corresponding volume % data in Table I), it can be seen that both the "elementary" and "particle agglomerate" sizes increase with the synthesis time. But the differential volume % curves for the synthesis time of 2 and 4 h exhibit multi-modal distributions with tails following the main peak. XRD results show that at this stage the degree of conversion is <80% (see Fig. 4). Namely, the hydrothermal product does not comprise fully crystallised perovskite PZT particles. About 10–20 area% of the hydrothermal product in the TEM micrograph is still in the amorphous state, and prone, therefore, to agglomeration. As the synthesis time increases to 6 h, the degree of conversion is increased to >80%. Consequently, the tendency to agglomerate decreases, and the modal "particle agglomerate" size becomes only slightly larger but the size distribution has become narrower and reasonably symmetrical.

The situation at a synthesis temperature of 300°C is even clearer, since the crystallisation of the PZT powders is more complete. The modal "elementary" particle size increases as the synthesis time increases. Interestingly, however, the modal "particle agglomerate" size remains almost constant, or perhaps decreases slightly, as the synthesis time increases. Careful examination of the particle size data demonstrates, in the case of the 4 and 6 h synthesis time, that although the "particle agglomerate" size distributions shift to larger particle sizes compared with the "elementary" particle size distributions, there is essentially no change in the distribution width. The striking difference is for the 2 h synthesis time, where the PZT powder is not fully crystallised (~80% conversion), making the powder prone to agglomeration. The "elementary" particle and "particle agglomerate" size distributions for the 2 h synthesis time are much wider than those for the 4 and 6 h synthesis time, and are asymmetric, especially the number % distribution.

4. Discussion

The particle size distribution and morphology of the PZT powders synthesised hydrothermally are determined by the particle nucleation and growth processes, to which both chemical and crystallographic aspects contribute. As shown in the present study, the nucleation of the perovskite PZT powder seems to be strongly dependent on the nature of mineraliser concentration, hydrothermal temperature and time.

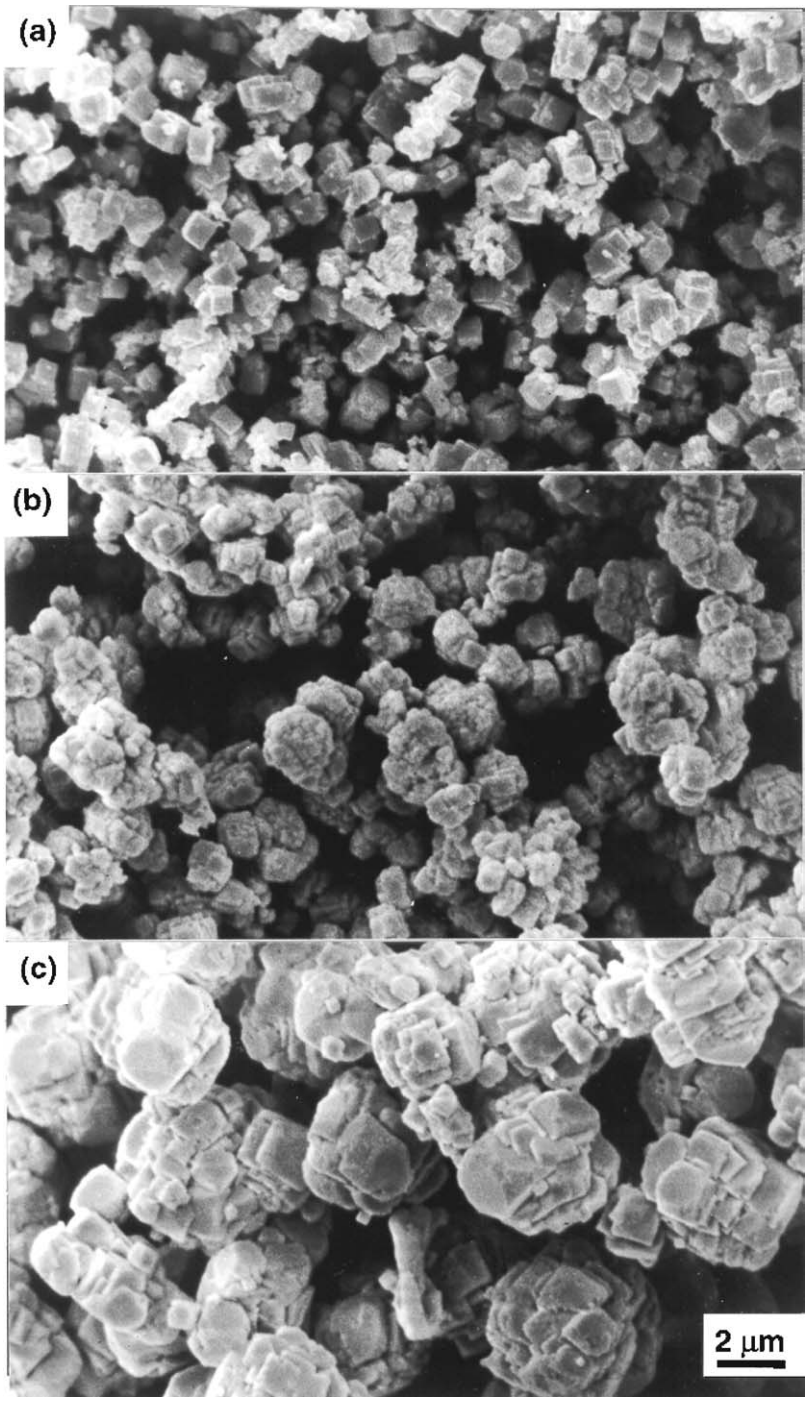

Figure 6 SEM micrographs of the PZT powders synthesised using different KOH concentrations at 300°C for 2 h: (a) 0.4 M, (b) 0.6 M, and (c) 1.0 M.

It has been reported that the precipitated titania and zirconia precursor gels tend to form polymeric chains such as $[Ti–O–Ti]_n$ and $[Zr–O–Zr]_n$ in preference to isolated Ti^{4+} or Zr^{4+} ions except at strong acidic conditions [14]. The Ti^{4+} or Zr^{4+} ion does not actually exist because of its high charge to ionic radius ratio. In the present work, the TIPT precursor modified by excess AcAc tends to form $[TiO(AcAc)_2]_2$ [15], and the coordination number of the Ti atom increases from four to six. Upon hydrolysis, the alkoxide groups are removed first, whereas the bidentate acetate ligands remain bonded to the Ti atom. During hydrothermal treatment, further condensation may occur, leading to the formation of acicular titania gels [16] and acicular titania crystals when the mineraliser concentration is low. Consequently, the solubility of the titania precursor gel will decrease with increasing hydrothermal temperature due to the further condensation from oligmers to polyhedra. On the other hand, the hydrous zirconia gel is probably composed of polymeric chains with unknown lengths, resulting from the incomplete hydrolysis of the acetate ligands [17]. Thus, the precursors for the PZT powders starting from zirconia-titania gel in two-step derived feedstock can be regarded as polymeric chains, leading to the formation of an entangled Ti–O–Ti and Zr–O–Zr network.

The precipitate from the lead acetate trihydrate dissolved in KOH solution will undergo following

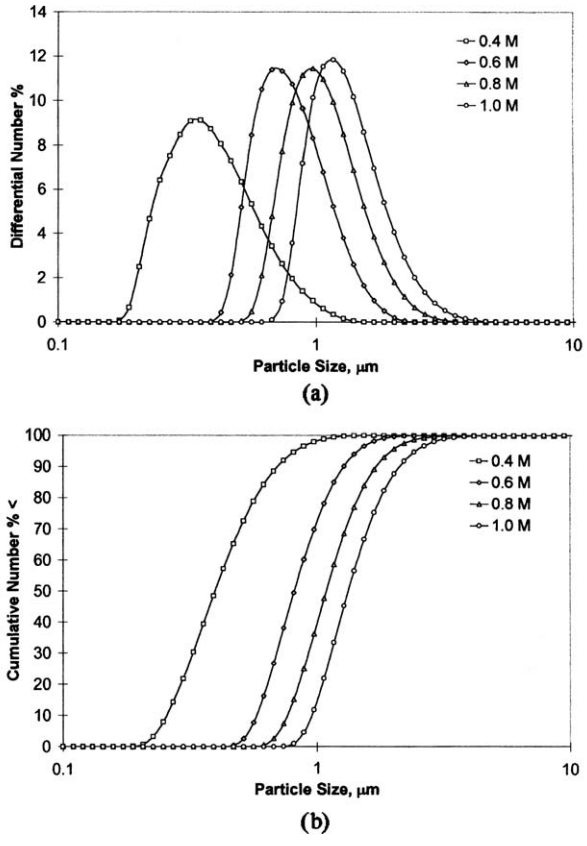

Figure 7 Effect of KOH molar concentration on the particle size distribution of the hydrothermal PZT powders synthesised at 300°C for 2 h: (a) differential number % and (b) cumulative num %<.

reaction resulting in the formation of hydrous lead oxide:

$$Pb(OAc)_2 \cdot 3H_2O(aq) + 2KOH(aq) \rightarrow PbO \cdot 3H_2O(s) + 2K(OAc)(aq) + H_2O(l) \quad (2)$$

However, the form of PbO produced can vary depending on the feedstock pH according to the following reaction equilibria [18].

$$PbO(s) + H_2O(l) \Leftrightarrow Pb^{2+}(aq) + 2OH^-(aq) \quad (3)$$

$$Pb^{2+}(aq) + H_2O(l) \Leftrightarrow PbOH^+(aq) + H^+(aq) \quad (4)$$

$$PbOH^+(aq) + OH^-(aq) \Leftrightarrow Pb(OH)_2(aq) \quad (5)$$

$$Pb(OH)_2(aq) + OH^-(aq) \Leftrightarrow HPbO^{2-}(aq) + H_2O(l) \quad (6)$$

$$Pb(OH)_2(aq) \Leftrightarrow Pb(OH)_2(s) \quad (7)$$

At a relatively low basic pH, reactions (3) and (4) are promoted, yielding Pb^{2+} and $Pb(OH)^+$. At a relatively high basic pH, reactions (5), (6) and (7) dominate. The neutral $Pb(OH)_2$ (aq) precipitates are in the form of $Pb(OH)_2$ (s). Fergusson [19] reported that, in the pH range 8 to 10, the dominant species is $PbOH^+$, which is replaced at about pH11 by $Pb(OH)_2$ (aq). At about pH 11.5, negative species such as $Pb(OH)^{3-}$ occur, which is also supported by the electrophoretic mobility results (see Fig. 9). In the present work, the pH of the feedstock solution ranges from about 11 to 13.7; therefore, the structure of the as-coprecipitated feedstock could be envisaged as being hydrated zirconia-titania gels bonded with unreacted acetate (OAc) and AcAc groups, together with surface-adsorbed $Pb(OH)^{3-}$ or ultrafine $Pb(OH)_2$(s).

Sengupta *et al.* [20] reported that heterometallic Ti–O–Zr bonding comprises only a small fraction of the network system since Ti–O–Ti and Zr–O–Zr linkages are formed preferentially through the homocondensation of M–OH and M–OR groups. The Pb cations do not participate in the bonding with the Ti and Zr atoms because Pb atoms only attain their regular coordination geometry at a higher temperature. Instead, they occupy random positions within the amorphous zirconia-titania gels. During hydrothermal synthesis,

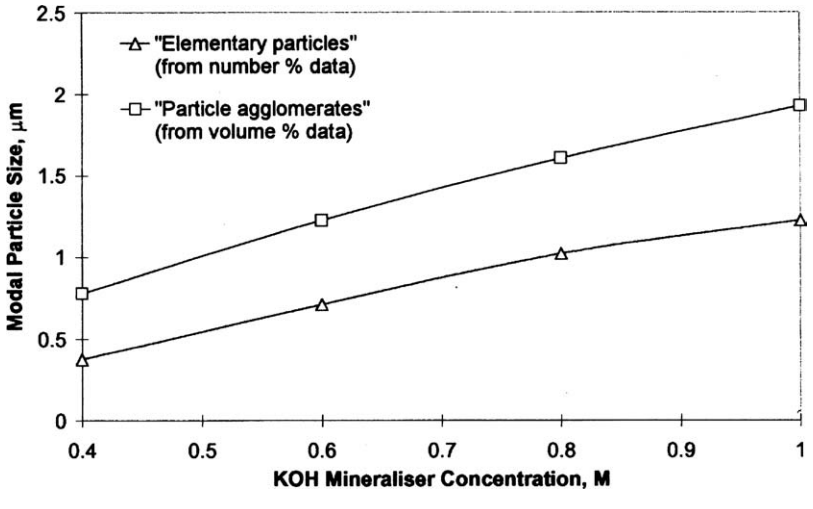

Figure 8 The relationship between the modal particle size in Fig. 7 and the mineraliser concentration for "elementary particles" and "particle agglomerates," respectively. The synthesis conditions are the same as in Fig. 7. The "elementary particles" sizes are represented by the number % data because they are less biased by the presence of a small number of large "particle agglomerates" than are the corresponding volume % data.

TABLE I Model particle size data for hydrothermal PZT powders synthesised at different temperature and time using 0.4 M KOH as the mineraliser

Synthesis temperature (°C)	Synthesis time (h)	Model particle size (μm)	
		Number (%)	Volume (%)
250	2	< 0.1	0.17
	4	0.26	0.70
	6	0.37	0.75
300	2	0.21	0.81
	4	0.41	0.72
	6	0.49	0.68

the PZT nuclei are mostly formed via an *in-situ* transformation process, in which the relatively mobile Pb species become incorporated within the zirconia-titania gel network, and eventually form the long-range ordered, i.e., crystalline cubic perovskite PZT structure through the expulsion of water. However, since zirconium has a tendency to adopt coordination numbers higher than six [21], it is likely that the initial zirconia-titania gel contains titanium with a coordination number of six and zirconium greater than six. The *in-situ* transformation of this mixed gel to a perovskite structure requires a greater degree of ordering of the lead and zirconium cations than of the lead and titanium cations because the coordination number of the zirconium has to be reduced. Therefore, some acicular lead titanate crystals were formed during the early stage of hydrothermal reaction at the minimum mineraliser concentration.

It should be noted, however, that the perovskite PZT structure may be formed only when the homogeneity of the zirconium and titanium atom distribution is achieved on a reasonable fine scale, although not necessarily at the molecular scale, either through pre-mixing of the zirconia and titania gels as in the present derived feedstock or through the dissolution and recrystallisation process which occurs at higher temperatures. Otherwise, a stable structure will always form from the heterogeneous mixtures of precursors as soon as the diffusion distances (related to temperature) are on the order of the heterogeneity scale. Upon increasing the homogeneity, the diffusion controlled reactions may transfer to nucleation-controlled reactions [22]. Lencka *et al.* showed experimentally that synthesis of a homogeneous solid solution PZT cannot be obtained with separate Ti and Zr precursors [7].

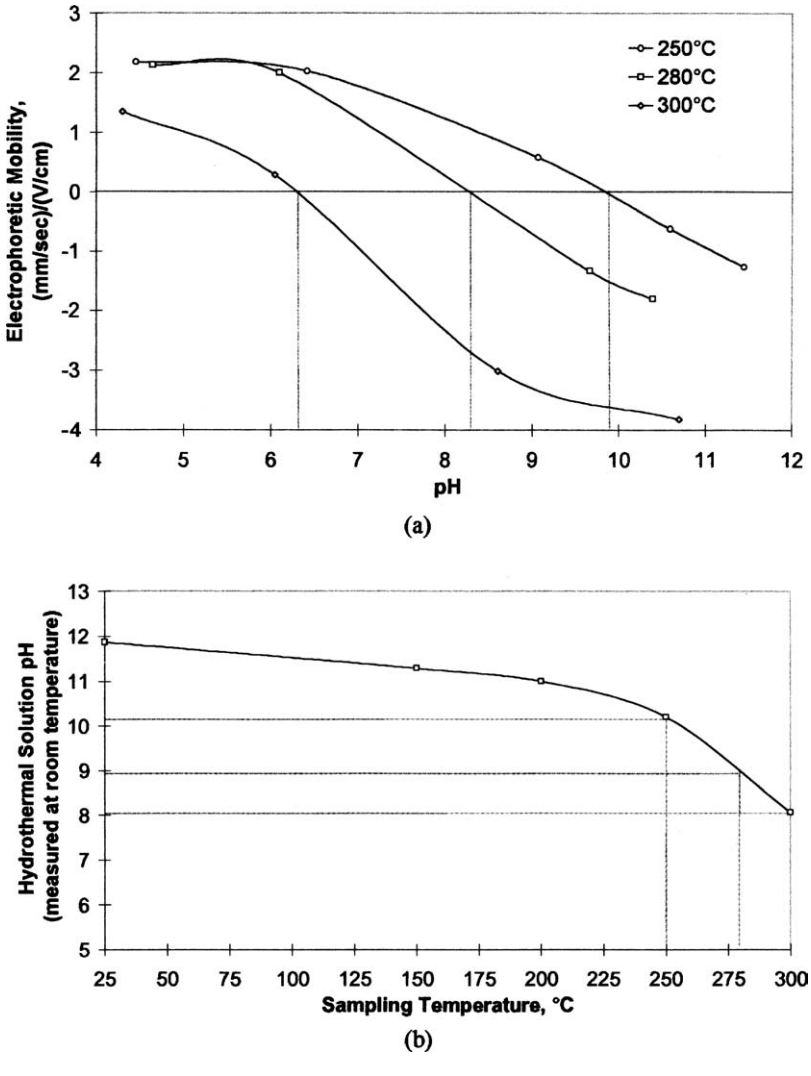

Figure 9 (a) Electrophoretic mobility of the hydrothermal PZT products extracted at different temperatures as a function of solution pH at room temperature, and (b) room temperature pH of the hydrothermal solution extracted at different temperatures during the hydrothermal process using 0.4 M KOH as the mineraliser.

The crystal growth stage, which follows crystal nucleation, can be rate-controlled by either the transport of polynuclear complexes to the growing particles or by their subsequent binding to the particle surface depending on the pH and ionic strength of the hydrothermal solution. It is well known that the oxide particles' surface becomes hydrated in an aqueous solution, resulting in a net surface electrostatic charge whose magnitude and sign depends on the solution pH. The resultant electrostatic potential field will repel like-charged ions but attract unlike-charged ions within the vicinity of the particles' surface, increasing their local concentration relative to that in the bulk solution in order to preserve electroneutrality. A diffuse electric double layer is formed around each particle [23]. If two particles approach each other, their double layers interpenetrate, generating a repulsive force between them. However, the van der Waals attractive potential is also operative, although over a much smaller distance from the particles' surface. The interaction of these long-range repulsive and short-range attractive potentials is described approximately by the Derjaguin, Landau, Verwey, and Overbeek (DLVO) theory [24]. Coagulation can occur on increasing the ionic strength of the solution and/or decreasing the surface potential of the particle.

Fig. 9a shows the electrophoretic mobility of the hydrothermal products extracted at various temperatures during their hydrothermal synthesis using 0.4 M KOH as a mineraliser, together with the two-step derived feedstock, as a function of their solution pH (adjusted by adding HNO_3 or KOH solution) at room temperature. The change in the hydrothermal solution pH during the hydrothermal synthesis process is shown in Fig. 9b. It is interesting to note that both the isoelectric point (IEP) of the hydrothermal PZT sols and the hydrothermal solution pH decrease simultaneously as the hydrothermal synthesis temperature increases. The IEP pH values of the hydrothermal PZT sols extracted at 250, 280, and 300°C are 9.8, 8.2 and 6.3, respectively (Fig. 9a). Correspondingly, the pH values of the filtrate solution extracted at 250, 280, and 300°C, although measured at room temperature, are 10.2, 8.8, and 7.8, respectively (Fig. 9b). This may imply that the PZT nuclei, as soon as they are formed, have a very strong tendency to coagulate throughout the synthesis process. Therefore, crystalline PZT particles with a particle size of about 200 nm are formed almost instantaneously at the minimum mineraliser concentration for perovskite PZT formation as observed by TEM. If the mineraliser concentration is low, the degree of supersaturation will be relatively low; hence, mononuclear growth will dominate [25]. Most of the particles, therefore, grow layer by layer, and the particle surfaces will be locally smooth at the molecular level. They thus take on a well-defined cubic shape, which corresponds to the basic crystal structure of the perovskite PZT. During the prolonged synthesis time, dissolution and recrystallisation will occur through the rearrangement of surface species to form smoother particle surfaces and a more uniform particle size distribution, as discussed previously. As the mineraliser concentration increases, both the degree of supersaturation of Pb and the ionic strength of the hydrothermal solution are increased. The primary PZT nuclei become colloidally unstable, and hence, prone to rapid coagulation, since the interaction potential barrier is reduced to a minimum by the salt ions, i.e., "ion crowding" occurs, causing compression of the electric double layer. The strong van der Waals attraction between a large number of the primary particles will thereby lead to polynuclear growth. The primary particles appear to aggregate or agglomerate together to form aggregates or agglomerates of cubic morphology PZT crystallites, as shown in Fig. 6b and c.

Therefore, in order to control the particle size and morphology of hydrothermally synthesised PZT powders, the mineraliser concentration used should be the minimum necessary for the specified mineraliser to ensure solely phase-pure perovskite PZT particle formation at the given synthesis temperature, where particle growth occurs via a mononuclear growth mechanism; this produces PZT particles with a well-defined cubic morphology. Increasing the mineraliser concentration will lead to polynuclear growth, with the result that the PZT particles, which are in fact agglomerates of cubic morphology PZT crystallites, exhibit an increased particle size and a morphology that is spherical rather than cubic. Increasing the synthesis temperature and prolonging the synthesis time can lead to a more symmetric particle size distribution due to the dissolution and recrystallisation process which occurs during the latter stage of synthesis.

5. Conclusions

The particle size and morphology of hydrothermally synthesised perovskite PZT powders can be controlled by the hydrothermal solution pH, in conjunction with the synthesis temperature and time, which influence the particle nucleation and growth mechanisms operating during hydrothermal processing. The base mineraliser is important as it assists in the nucleation of perovskite PZT particles. The minimum KOH concentration required should be twice as the input Pb precursor concentration to the formation of perovskite PZT powders. At such a high pH condition (>pH 11), PZT nuclei were mainly formed via *in-situ* transformation mechanism. The PZT nuclei, however, tend to coagulate to form cubic particles of about 200 nm almost instantaneously. As the KOH concentration increases, the tendency of the cubic "elementary" PZT particles to coagulate to form "aggregate" during the particle growth stage is increased because of the higher ionic strength of hydrothermal solution. Longer synthesis time enables further particle growth with a narrowing of the size distribution and/or a tendency towards a more equiaxed particle morphology because of the dissolution/precipitation mechanism operating during the later synthesis stage and higher synthesis temperatures reduce the extent of agglomeration but the "elementary" particles grow larger.

Acknowledgment

One of the authors (B. Su) wishes to acknowledge the financial support from the ORS award and the department.

References

1. F. F. LANGE, *J. Amer. Ceram. Soc*. **72** (1989) 9.
2. W. J. DAWSON, *Amer. Ceram. Soc. Bull*. **67** (1988) 1673.
3. R. E. RIMAN, in "High-performance Ceramics," edited by R. Pugh and L. Bergstrom (Marcel-Dekker, New York, 1993) p. 29.
4. T. R. N. KUTTY and R. BALACHANDRAN, *Mater. Res. Bull*. **19** (1984) 1479.
5. T. ICHIHARA, T. TSURUMI, K. ASAGA, K. H. LEE and M. DAIMON, *J. Ceram. Soc. Jpn. Intel. Ed*. **98** (1990) 155.
6. H. CHENG, J. MA, B. ZHU and Y. Cui, *J. Amer. Ceram. Soc*. **76** (1993) 625.
7. M. M. LENCKA, A. ANDERKO and R. E. RIMAN, *ibid*. **78** (1995) 2609.
8. M. TRAIANIDIS, C. COURTIS and A. LERICHE, *J. Euro. Ceram. Soc*. **20** (2000) 2713.
9. E. SOVACI, A. DOGAN, J. ANDERSON and J. H. ADAIR, *Chem. Eng. Comm*. **190** (2003) 843.
10. K. C. BEAL, "Advances in Ceramics, Ceramic Powder Science" (The American Ceramic Society Inc., 1987) Vol. 21, p. 33.
11. S. B. CHO, M. OLEDZKA and R. E. RIMAN, *J. Cryst. Growth* **226** (2001) 313.
12. Y. OHBA, T. RIKITOKU, T. TSURUMI and M. DAIMON, *J. Ceram. Soc. Jpn*. **104** (1996) 6.
13. B. SU, T. W. BUTTON and C. B. PONTON, *Rev. High Press. Sci. Tech*. **7** (1998) 1348.
14. C. F. BAES JR. and R. E. MESMER, "The Hydrolysis of Cations" (Krieger Publishing Company, Florida, 1986) p. 147.
15. G. D. SMITH, C. N. CAUGHLAN and J. A. CAMPBELL, *Inorg. Chem*. **11** (1972) 2989.
16. D. HENNINGS, G. ROSENSTEIN and H. SCHREINEMACHER, *J. Euro. Ceram. Soc*. **8** (1991) 107.
17. D. V. LUEBKE, US Patent, 3,442,817 (1969).
18. E. J. MARGOLIS, "Chemical Principles in Calculations of Ionic Equilibria" (Macmillan, New York, 1966).
19. J. E. FERGUSSON, "The Heavy Elements: Chemistry, Environmental Impact and Health Effects" (Pergamon, Oxford, 1990).
20. S. S. SENGUPTA, L. MA, D. L. ADLER and D. A. PAYNE, *J. Mater. Res*. **10** (1995) 1345.
21. I. LAAZIZ, A. LARBOT, A. JULBE, C. GUIZARD and L. COT, *J. Solid State Chem*. **98** (1992) 393.
22. P. BARBOUX, P. GRIESMAR, F. RIBOT and L. MAZEROLLES, *ibid.* **117** (1995) 343.
23. R. J. HUNTER, "Zeta Potential in Colloidal Science: Principle and Applications" (Academic Press Ltd., London, 1981) p. 22.
24. J. N. ISRAELACHVILI, "Intermolecular and Surface Forces" (Academic Press Ltd., London, 1992) p. 248
25. A. C. PIERRE, *Amer. Ceram. Soc. Bull*. **70** (1991) 1281.

Received 10 December 2003
and accepted 23 June 2004